

## A COMBINATORIAL BRIEF INSIGHT INTO MICROBE INDUCED CORROSION OF GALVANIZED STEEL AND ITS ALLEVIATION WITH ECO-FRIENDLY INHIBITORS

R. Sharmil Suganya\*, Stanelybritto Maria Arul Francis and T. Venugopal

Government College of Engineering, Salem-11, Tamil Nadu, India

(Received June 10, 2024; Revised October 29, 2024; Accepted November 1, 2024)

**ABSTRACT.** This study primarily focused on the influence of *Reullia tuberosa* extract in alleviating *Staphylococcus aureus*, *Klebsiella pneumonia*, and *Bacillus subtilis*-induced corrosion on the metal samples. Nyquist plots and impedance investigations were carried out to warrant the nature of green inhibitors in controlling biocorrosion. The corrosion patterns in certain pitted zones revealed a strong correlation between the chemical composition of the metal surface and microbial metabolites based on analytical studies. The presence of microbial metabolites resulted in an increase in the porosity and permeability of the metallic surface, thereby altering the structural composition of the surface. The highest concentration of plant extract in inhibiting the microbial corrosion was identified to be 30 ppm in all three microbes. Weight loss of the coupons that were immersed in the control solution showed that corrosion rates went up for a short time but then went down after the inhibitor was added. The green inhibitors were able to alleviate the development of biofilm in the pitted areas. Analytical outcomes warranted that the green inhibitors successfully regulated the formation of microbial growth products. This study found that phytoconstituents in plant extracts effectively stopped corrosion from happening and also stopped microorganisms and biofilm from growing.

**KEY WORDS:** Microbial-induced corrosion, Biofilm, Plant extracts, *Reullia tuberosa*, Galvanized steel, Green inhibitors.

### INTRODUCTION

Metal oxides are prone to disintegration through rusting and deterioration, transforming them into corrosive substances that pose a significant risk to the industry. This can result in system failures, damaged goods, reduced heat transfer efficiency, increased operating expenses, compromised machinery frameworks, leaks, and decreased output from power plants. Corrosion can also hinder the transportation of water and reduce the operational efficiency of the entire water system, leading to severe financial consequences. Heating, ventilation, and air conditioning (HVAC) operations rely on cooling towers, essential equipment for direct and indirect heat removal. These towers utilize the evaporation process to convert heated water into cool water at specific temperatures. The system recycles industrial wastewater by extracting excess heat from heat transfer surfaces, allowing it to pass through heat exchangers. Cooling tower structures are designed to facilitate evaporation, absorbing heat and releasing it into the air. The evaporated heat is then transformed into water droplets at the top of the towers, collected, and reused within the industry.

Cooling towers mitigate a vast amount of generated heat from equipment during operational processes in the industrial sector. These towers play a crucial role in regulating constant machinery temperatures and dissipating heat throughout the course of work. Various influencing variables, such as dissolved inorganic salt concentration, surrounding temperature, pH, moisture, and microbial growth, collectively favour the development of corrosion in these structures. Corroded spots act as stress concentrators, inducing component breakdown, systemic instability,

---

\*Corresponding authors. E-mail: [sweetsharmil@gmail.com](mailto:sweetsharmil@gmail.com)

This work is licensed under the Creative Commons Attribution 4.0 International License

and ultimately catastrophic collapse. Due to extreme conditions and operational circumstances, cooling towers are also vulnerable to failure over time, frequently leading to overall problems [1]. Literature has reported that prolonged exposure to atmospheric acidic environments leads to the adsorption and diffusion of chloride ions onto the surfaces of cooling towers. Over time, corrosion pits may appear, leading to the acceleration of corrosion. The electrochemical and chemical mechanisms of corrosion involve the reduction and oxidation of potential on the outermost layers of metal. Mild steel (MS), characterized by low carbon content and durability at an affordable cost, is frequently used in cooling tower installations. Cooling towers are susceptible to thermal robustness issues, structural deterioration, moisture retention, and the harbouring of microbes within the tower. The development of corrosion on the surface may lead to operational shutdowns. Organic or inorganic coatings are applied to the surface to prevent the superficial development of corrosion and reduce the corrosion rate.

Microbiologically influenced corrosion (MIC) is the concept adopted to decipher the microbial mechanism and its influence on the rate of progression of corrosion processes on metals and non-metallic surfaces. Corrosion is significantly influenced by microbes, especially on metal surfaces. Biofilms are developed by a plethora of bacterial populations along with secretions. These films form when bacteria accumulate on metals, creating various microenvironments, thereby modifying the wettability and electrostatic charge of the hard, solid surface, making it easier for bacteria to colonize the outermost layer. The pH, dissolved chemicals, oxygen concentration, exposure duration, and location of the biofilm are not constant. The establishment of an organic compound and an inorganic ion-rich boundary layer on a solid surface is the initial stage in the formation of a biofilm. This layer attracts microorganisms, and over time, additional microbes move closer to it, developing a biofilm layer composed of fluids, microbes, and other environmental components. This process damages surfaces and accelerates corrosion rates [2]. Corrosion begins and develops beneath this biofilm, causing localized corrosion. This localized corrosion, over an unmonitored period of exposure, subsequently leads to the development of metal wall perforations [3]. Rapid industrialization mandates a paradigm shift towards cost-effective, non-toxic, and biodegradable alternatives to hazardous corrosion inhibitors [4]. Plant extracts have quickly gained popularity as safer alternatives to these organic and inorganic inhibitors in recent years [5].

Plant extracts derived from plant sources act as potential inhibitors against corrosion on metal surfaces. Organic phytochemicals, such as terpenoids, and other hydrocarbons, have an affinity to be adsorbed over the metal surface and exert their antibacterial properties against a variety of microorganisms. There is a paradigm shift towards utilizing plant extracts as green corrosion inhibitors, and it has proven to be a promising topic in this research field [6]. Three microorganisms, particularly *Staphylococcus aureus*, *Klebsiella pneumonia*, and *Bacillus subtilis*, have been selected to evaluate the effects of microorganisms on corrosion resulting from their interactions with a metallic surface. Investigations were carried out to examine the impact of extracts from *Reullia tuberosa* on bio corrosion. The development of sustainable materials is essential for reducing the harbouring of microorganisms on metallic surfaces. To minimize adverse impacts on the ecosystem and prevent corrosion on the metallic surface, environmentally conscious formulations are recommended. To achieve high inhibitory effectiveness, a multimodal technique integrating metal surface interactions and microbial chemistry has been adopted to decipher the insights of the inhibition of microbial corrosion by plant extracts.

## EXPERIMENTAL

### *Collection of cooling tower water (CTW) and processing of steel coupons*

The cooling tower water was collected in sterilized bottles (autoclaved) and placed in an icebox. It was then brought from the Mettur Thermal Power Station for laboratory purposes. The average

pH value was with a range of 7.8–8.3. The Total dissolved substance (TDS) varied from 138 to 200 mg L<sup>-1</sup>. The average temperature of the cooling tower water was 27–30 °C. Fine chemicals used for microbiological assays were procured from Himedia and were of analytical reagent grade. The mild steel coupons were polished to achieve a final surface finish, cleaned with ethanol, and air dried in a desiccator. The dry coupons were weighed before and after experimental studies. Weight loss measurements were carried out on a mild steel coupon (6 cm x 1 cm), followed by pickling treatment to clean the dirt, and then weighed. Polarisation and impedance analysis were carried out using mild steel coupons (1 cm x 1 cm) without cleaning by pickling solution or washing with water.

#### *Microbial culture and preparation*

Each bacterial strain was sub-cultured in LB broth at 37 °C. A working stock of 107 CFU/mL of bacterial cells was prepared in sterile water after measuring the absorbance using a spectrophotometer. Three bacterial strains—*Staphylococcus aureus*, *Bacillus subtilis*, and *Klebsiella pneumonia*—were selected. The microbial strains were gifted by Department of Microbiology, Periyar University, Salem, and Tamil Nadu. The chosen strains were subcultured and maintained in Luria Bertani (LB) Broth following standard recommendations [7]. One milliliter of the microbial culture with a cell density of 107 CFU/mL was seeded into 100 mL of sterile Luria Bertani Broth and incubated in the shaker incubator for 50 min, followed by incubation in the temperature-controlled incubator at 37 °C for 18 hours.

#### *Soxhlet extraction*

The flowers of *Ruellia tuberosa* were obtained from the surroundings. These were ground to a fine powder, sieved, and then used for extraction. Ten grams of the powdered sample were placed inside a thimble and inserted into the Soxhlet extractor. Two hundred mL of ethanol was added to the 10 g powdered sample, and extraction of the oil was carried out for 48 hours as per the standard procedure by maintaining a solute-solvent ratio of 1:10. The refluxing temperature was 55 °C. After extraction, residual ethanol was removed using a rotary evaporator, leaving the essential oil as the end product. The essential oil was stored in an amber bottle for further analysis, including gas chromatography-mass spectrometry (GC-MS) analysis.

#### *Well diffusion method*

The well diffusion assay was performed according to standard recommendations [9]. For the solidified LB Agar plates, 100 µL of bacterial suspension was spread using a sterilized L rod into respective petri plates. Seven-millimetre diameter wells were made in the agar medium using a sterile cork borer (7.5 mm) and then filled with the green inhibitors at three different concentrations (10, 30, and 50 µL), respectively. Di-methyl sulfoxide (DMSO) and Amoxicillin were used as controls. The plates were incubated for 24 hours, and the zones of inhibition were measured using digital vernier callipers to evaluate the minimum inhibitory concentration (MIC).

#### *Weight loss method*

Weight loss study was performed based on standard protocol with slight modifications and recommendations [10]. The control system comprised a polished mild steel coupon immersed in a conical flask filled with 400 mL of cooling tower water. The microbial system included sterile Cooling Tower Water (CTW) (400 mL), nutrient broth (1% w/v), and 1 mL each of three microbial cultures without mild steel coupons. A sterile polished mild steel coupon was immersed in 400 mL of sterile cooling tower water, serving as the control in this context. The corrosion

inhibitor reaction mixture consisted of sterile CTW (400 mL), nutrient broth (1% w/v), and 1 mL each of three microbial cultures, which were inoculated in 500 mL conical flasks. Sterile polished mild steel coupons were then dipped into the sterile medium in a controlled inoculation chamber. Subsequently, various concentrations of plant extracts, each with 10, 20, 30, 50  $\mu\text{L}$ , were added to the respective flasks. After the appropriate treatment, the mild steel coupons were taken, air-dried, and weighed to measure the weight loss due to the corrosion reaction.

#### *Corrosion analysis*

Corrosion rate analysis was conducted for triplicates of each system. Every week, the coupons were extracted from the conical flasks, autoclaved, and weighed. Studies on weight loss measurement were performed by immersing the coupons in the pickling solution (1000 mL, 0.1 N hydrochloric acid containing 20 g (w/v) antimony trioxide and 50 g (w/v) of stannous chloride) at room temperature for 25 min. XRD and SEM analysis were conducted on the acid-treated corroded coupons. After three weeks, the coupons were removed from their respective systems, and the corrosion products were scraped from each metal and analysed [10].

#### *Electrochemical studies*

Electrochemical studies were conducted using an electrochemical workstation (Model CH 1608 D/E Series) consisting of a platinum electrode and a reference electrode (saturated calomel with Ag/AgCl). Mild steel coupons (1.0 x 1.0  $\text{cm}^2$ ) were used for conducting electrochemical studies with a three-electrode cell [10].

#### *X-Ray diffraction (XRD) spectroscopic analysis*

Metal scrapped from the mild steel was characterized using an X-Ray diffraction instrument (Wilcox 132 XRD analyzer) with a maximum power of 12 KW (60 kV and 200 mA) [11].

#### *Scanning electron microscopy (SEM)*

The corrosion products were scraped, crushed into a fine powder, mounted on aluminium holder stubs using double sticky carbon tape, and coated with Au/Pd in a BIORAD Polaran E5400 High-Resolution sputter coater. They were examined in a ZEISS Scanning Microscope (Elvis 15, Germany) at 15 KV. The SEM images were analysed to identify microstructural variations [12].

#### *Fourier transform-infrared (FTIR) analysis*

The Fourier transform-infrared spectra of the oil sample were obtained using a Perkin Elmer Model. The absorbance was measured in the wavelength range of 4000  $\text{cm}^{-1}$  to 400  $\text{cm}^{-1}$  with a resolution of 4  $\text{cm}^{-1}$ . The samples were pelleted using KBR, and the pellets were used for further analyses [13].

#### *Gas chromatography – mass spectrometric (GC-MS) analysis*

Gas chromatography mass spectrometry (GC-MS) analysis was performed using Bruker 45X (GC) and SC-ION (MS) equipment equipped with a mass detector and analyzed in a connected workstation. Helium carrier gas (70 °C and 5 min of holding time) was used in the capillary column (15 m in length). One microliter of the sample was injected into the GC column at a flow rate of 1 mL/min, maintaining a 45-minute total run time. The separated metabolite mass spectra were recorded (70 eV), and the peaks of GC-MS were compared with the National Institute of

Standards and Technology (NIST) database, identifying the metabolites. The peaks in the GC-MS of the ethanol extract indicated the presence of bioactive compounds [14].

## RESULTS AND DISCUSSION

The presence of microbiological consortia, where various species of microbes coexist within the biofilm framework, has led to potentially detrimental corrosion on the metallic surface [15]. A variety of microbes, including sulphate-reducing, metal-oxidising, metal-reducing, acidic, slime, hydrogen-consuming, and hydrogen-producing, aerobic, and anaerobic microorganisms, contribute to the bio-corrosion process [16]. Multiple species coexist and cause the corrosion process because of the activation of a plethora of biochemical processes at the oxic-anoxic transition zones, negatively and directly impacting both human health and commercial operations [17].

### *Anti-microbial studies*

In the current investigation, the well diffusion method is used as the primary testing approach to determine if the selected three plant extracts could inhibit the studied microbes, in vitro. Table 1 illustrates the zones of inhibition by essential oils. The plant inhibitor, *Ruellia tuberosa* was used at different concentrations, namely T1, T2, T3 (10, 30, and 50  $\mu\text{L}$ , respectively), while 50  $\mu\text{L}$  of DMSO and sterile amoxicillin discs acted as negative and positive controls, respectively. Studies reported that phyto-constituents present in *Ruellia tuberosa* [18] exhibited antimicrobial activity, inhibiting the formation of biofilm. However, the current experiments revealed no significant variation among the three concentrations (T1, T2, and T3), respectively. The plant extract at 30 ppm was reported to inhibit better in terms of a higher zone of inhibition. Table 1 depict the Diameters of clear zone of inhibition by well diffusion method.

The antibacterial activities of essential oils stem from their secondary metabolites, which interact with the lipids in microbes' cell membranes, causing metabolic impairment and cellular death. Secondary metabolites released by these microbes play a vital role in both the cellular growth and death. These secondary metabolites prevent bacteria from growing by disrupting the framework of cell membranes and the enzymatic machinery [19]. The integrity of cells, as well as the movement of nutrients, energy, and communication between the cells and their surroundings, depends on the cell membrane. Macromolecular substances such as proteins and nucleic acids seep out when the cell membrane breaks down [20], thereby contributing to the inhibition of the microbial growth or cell death, exhibiting anti-bacterial properties.

Table 1. Diameters of clear zone of inhibition by well diffusion method.

Plant extract	Microbes	Negative control (mm)	Positive control (mm)	T1 (10 $\mu\text{L}$ ) (mm)	T2 (30 $\mu\text{L}$ ) (mm)	T3 (50 $\mu\text{L}$ ) (mm)
<i>Ruellia tuberosa</i>	<i>S. aureus</i>	11	13	11	11	12
	<i>B. subtilis</i>	9	11	11	12	12
	<i>K. pneumoniae</i>	11	12	11	11	12

### *Surface analysis*

The corrosion products were collected, crushed into a fine powder, and utilized for X-ray diffraction spectroscopy (XRD) and Fourier transform infrared spectroscopy (FTIR). The surface film was scraped using a sterile spatula and dissolved in methanol for further analysis.

### SEM analysis

SEM images of mild steel coupons exposed to microbe-infected cooling tower water illustrate the formation of biofilms leading to corrosion. Different concentrations of the cells facilitate bacterial adhesion to the steel surface, allowing the development of biofilms containing exopolysaccharides (EPS) to act as a diffusion barrier for corrosive substances. The cells that are localized with higher oxygen concentration, variability in the thickness of the biofilms, and irregular distribution of EPS and other corrosion by-products expedite the corrosion process. The structural composition and characteristics undergo modification during the corrosion process due to chemical or electrochemical interactions between the exposed surface and the surrounding environment [21].

The corrosion pattern appears highly heterogeneous, with corrosion debris accumulating on the metallic surface. Additionally, the microbial presence indicates a strong interaction with the surface, leading to the formation of pits in localized regions along with noticeable surface scratches. SEM analysis reveals the presence of crevices and a high density of accumulation over the metal surface.

Literature have reported that microbe-induced corrosion initiation occurs in three stages: physical adherence of the microbial consortium, harbouring and release of corrosive metabolites, and finally, depolarization of the metal surface at the hydrophobic substrate's surface [22]. The heightened corrosivity under biological conditions results from the harbouring and growth of microbial consortia, subsequently generating and releasing corrosive metabolites into the surrounding areas. The released corrosion metabolites alter the structural components of the material under investigation, enhancing the porosity and permeability of more corrosive materials into the pitted zone [23].

Experimental results demonstrate formation of microbial biofilm over *Ruellia tuberosa* treated mild steel. The plant extracts (corrosion inhibitors) exhibit a significant effect on the metal surface, hindering the disintegration. The three microbes *S. aureus*, *B. Subtilis* and *K. pneumonia* induced corrosion was found to be effectively inhibited by plant extract. Figure 1 (a) shows the SEM image of the control without microbes, while Figure 1 (b-d) displays control SEM images of the three microbe-treated mild steel samples (B: *S. aureus*, C: *B. subtilis*, and D: *K. pneumoniae*) without plant extract.

### FTIR

The samples were scrapped from the corroded mild steel surface and subjected to FTIR analysis. The corroded samples were scrapped from the MS coupons for FTIR spectra (Figure 2). The peak observed around  $3409\text{ cm}^{-1}$  is attributed to the hydroxyl groups (-OH group) of surface-bound water molecules. Peaks at  $1631\text{ cm}^{-1}$  may be associated with the bending vibration of absorbed water, surface hydroxyl, and O-H stretching mode. Peaks at  $518\text{ cm}^{-1}$  and  $620\text{ cm}^{-1}$  are likely due to the presence of  $\text{Fe}_2\text{O}_3/\text{FeS}$  [24]. The FTIR spectrum reveals several bands below  $600\text{ cm}^{-1}$ , linked to functional groups of alkaloids, flavonoids, and organic acids in *Ruellia tuberosa*. The presence of bacterial plasmid is a significant factor in the biofilm production of many bacterial strains. The hydrophobicity of the cell surface plays a crucial role in facilitating interactions among polar and non-polar functional groups. Moreover, the mobility of the microbe over the metal contact surface is a critical factor in the biofilm development process [25].

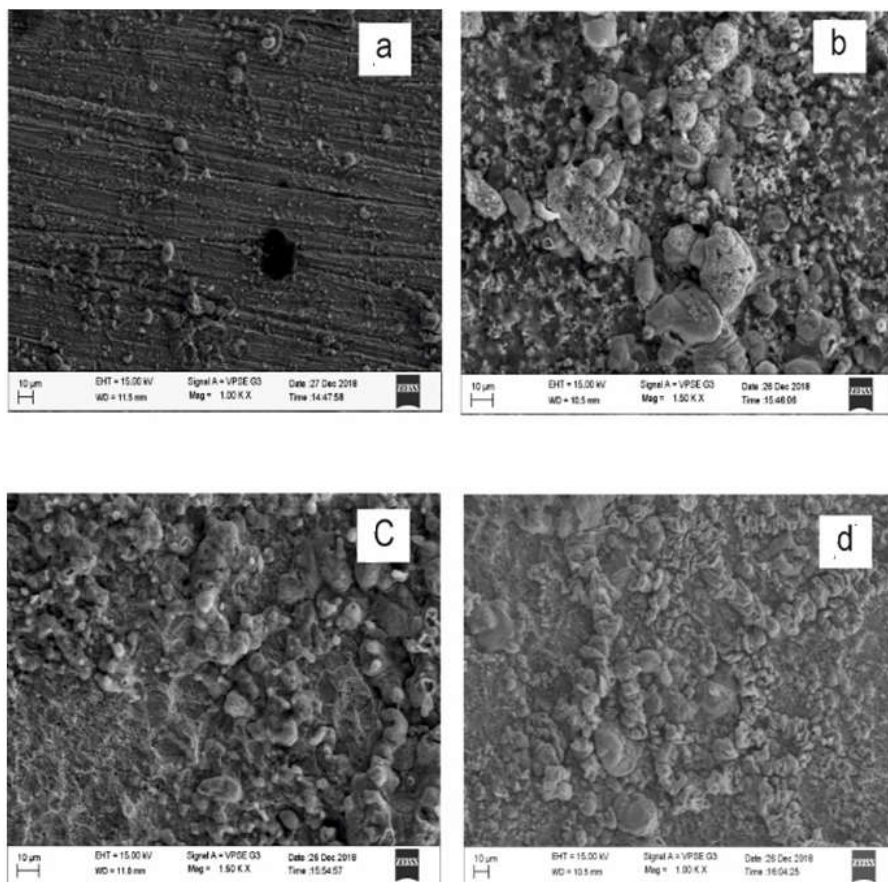


Figure 1. SEM analysis of control (a) and three microbe coated mild steel structures (b-d).

#### XRD analysis

The microbial induced corrosion pattern and its inhibition by the plant extracts of the specimens was assessed. The mild steel surface was scrapped and investigated by XRD. Figure 3 (A-C) represents XRD analysis of the bio-corrosion process due to three microbes (*S. aureus* (A), *B. subtilis* (B) and *K. pneumonia* (C)). The XRD pattern of the pure mild steel treated in cooling tower water (CTW) represents peaks pertaining to iron hydroxide (FeOOH) and ferrous sulphide (FeS) [26]. Corrosion products (FeS) is found deposited over the surface of the mild steel treated with CTW. In case of addition of bio corrosion inhibitor to the microbe induced corroded mild steel, disappearance and re-appearance of new peaks were reported due to the inhibition of the biofilm formation over the outer surface of the mild steel. It seems that the peaks attributed to iron oxides, such as Fe<sub>3</sub>O<sub>4</sub> and FeOOH, are disappearing. This demonstrates that the metal's surface is totally insulated from corrosion and that there is no indication of iron oxide present in the protective coating. Inhibitors, including carbon, nitrogen, oxygen, and phytochemical substances, may form a protective layer and minimise the iron peaks on metals [27]. Figure 3 represents the XRD analysis of the microbial induced bio-corrosion process of *S. aureus* (A), *B. subtilis* (B) and *K. pneumoniae* (C) treated *Reullia tuberosa* with along with control.

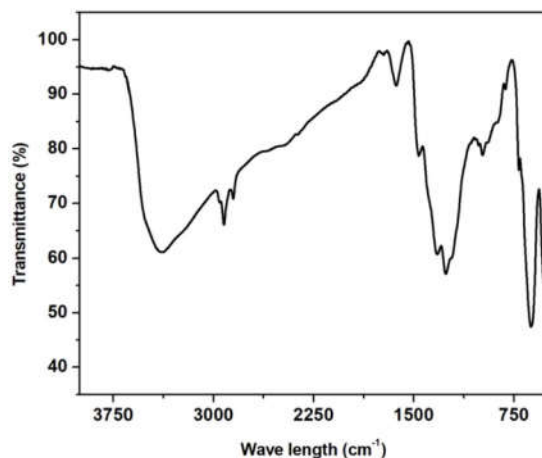


Figure 2. FTIR analysis of the corroded samples of *Reullia tuberosa* treated mild steel.

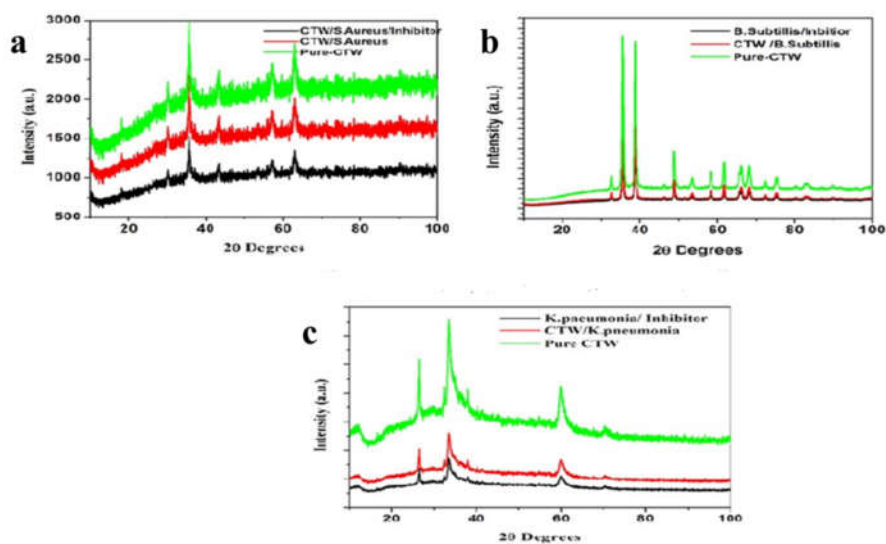


Figure 3. XRD analysis of the microbial induced bio-corrosion process of *S. aureus* (a), *B. subtilis* (b) and *K. pneumoniae* (c) treated *Reullia tuberosa* with along with control.

#### GC-MS analysis

Figure 4 represents the GC-MS analysis of the plant extracts, *Reullia tuberosa* which shows the presence of clindamycinin, benzoic acid, 2-fluoro-, 4H-Pyran-4-one, 2,3-dihydro-3,5-dihydroxy-6-methyl-, 7-Allyloxy-4-methylcoumarin in *Reullia tuberosa* (Table 2) [28]. Literatures have reported that the secondary metabolites play a vital role as a surface protective coating, attributing to the inhibitory effect on the bacterial growth [29].

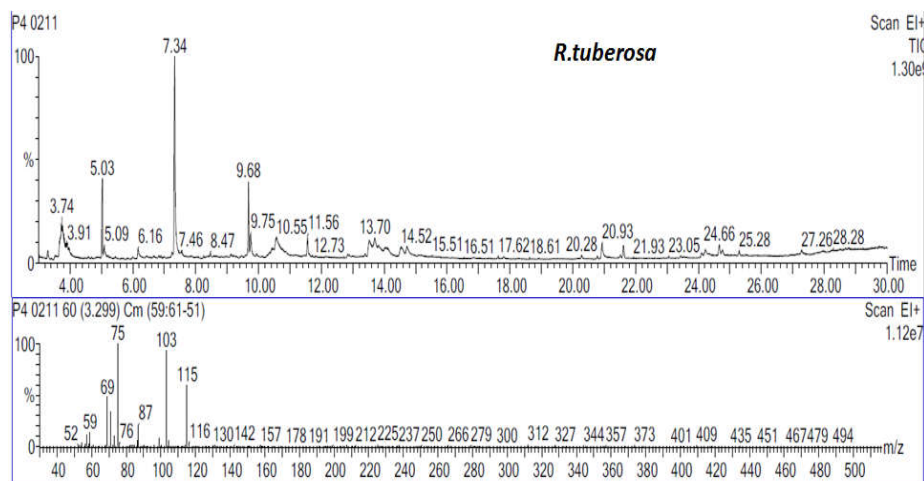
Figure 4. The GC-MS analysis of *Reullia tuberosa*.

Table 2. Constituents of inhibitors analysed by GC-MS.

Retention time	Compound	Area %
3.299	Butane, 1,1-diethoxy-3-methyl-	0.563
3.524	1-Butyl(dimethyl)silyloxypropane	0.330
3.744	Glycerin	8.244
3.899	Formic acid, 2-propenyl ester	1.775
3.979	Methional	1.476
5.029	Propane, 1,1,3-triethoxy-	3.571
5.089	Clindamycin	1.321
5.224	Benzoic acid, 2-fluoro-	0.340
6.165	4H-Pyran-4-one, 2,3-dihydro-3,5-dihydroxy-6-methyl-	1.096
7.245	7-Allyloxy-4-methylcoumarin	0.449
7.335	5-Hydroxymethylfurfural	14.453
7.525	d-Galactono-1,4-lactone, 5,6-O-(ethylboranediyl)-	0.555
7.560	Glycan 6-Sialylgalactose	0.784
7.665	Acetylhydrazide, 2-(4-fluorophenoxy)-N2-(4-allyloxybenzylideno)-	0.323
7.865	2,3-Diethoxy-propionic acid, ethyl ester	0.309
8.466	5-Acetoxyethyl-2-furaldehyde	0.298
9.126	Dodecanoic acid	0.326
9.681	2,3-Dipropyl-cyclopropanecarboxylic acid, ethylester	2.696
9.746	Trioxsalen	1.118
10.361	1,3-Dioxolane-2-propanol, 2,4-dimethyl-	0.523
10.421	Benzaldehyde, 2-hydroxy-6-methyl-	1.489

#### Electrochemical impedance

The electrochemical impedance study is done in the absence and presence of microbes and inhibitors in the cooling tower water systems [30]. Based on impedance spectral analysis, additional influential parameters, such as charge transfer resistance ( $R_{ct}$ ) and double-layer capacitance ( $C_{dl}$ ), are computed [6]. Table 3 (a) presents the impedance parameters derived from Nyquist plots. The susceptibility of mild steel to various ecosystems exhibited significant

variation [31]. With an increase in the exposure period, the impedance of steel has showed variation and an upward trend. This increase indicated that steel underwent a regulated corrosion rate in sterile culture media, with variability likely driven by the corrosion product. The disturbance in the system could be attributed to the negative value of the phase angle at higher frequencies. High frequencies revealed the presence of a capacitive semicircle, possibly resulting from corrosion product deposition and biofilm growth on the surface layer. A small capacitive loop observed at low frequencies may be explained by the development of metallurgical dissolution influenced by charge transfer mechanisms.

From the Nyquist plots, impedance parameters such as solution resistance, charge transfer resistance, and double-layer capacitance values were obtained. The inhibition efficiency was calculated by comparing inhibited and uninhibited charge transfer resistance [32]. Nyquist plots displayed single semicircles as capacitive loops in the high-frequency range, indicating charge transfer resistance both in the presence and absence of an inhibitor (plant extracts). Previous studies have shown a linear relationship between the semicircle and biofilm load, suggesting that biofilm adherence to the mild steel surface obstructs charge transfer and reduces the corrosion rate [33].

In microbiological ecosystems, interactions between solid materials and fluids are influenced by enzymes and metabolites produced by bacteria. These by-products can alter the electrochemical characteristics of the outermost layer, affecting the corrosion rate and the surface's tendency to receive or release electrons [34]. Biofilms are structurally and functionally stable as they release naturally occurring polymers. Microorganisms in bio-electrochemical systems play a role in creating intricate biofilms on solid surfaces [35]. Extracellular polymeric substances encapsulate components such as exo-polysaccharides, proteins, genetic materials, and metabolites secreted by these microorganisms. These molecules are closely associated with extracellular polymer synthesis and are essential for the formation of biofilm deposits.

There is a linear correlation with the biofilm formation and the Nyquist plot diameter. Generally, a larger semicircle diameter in Nyquist plots usually indicates higher electrical resistance at the metal–solution interface, which implies lower corrosion rates. The *Reullia tuberosa* extract was efficient in alleviating microbe induced corrosion, by inhibiting the biofilm formation, under similar operating conditions. Increasing order of the microbial inhibition by the extract was reported to be *Staphylococcus aureus* > *Klebsiella pneumoniae* > *Bacillus Subtilis*. It is noted that phyto-constituents present in *Reullia tuberosa* [18] exhibited anti-microbial activity, inhibiting the formation biofilm (Figure 5(a-c)). Under optimal operational conditions, the extract from *Reullia tuberosa* effectively minimized microbe-induced corrosion by impeding the development of biofilms (Figure 5(a-c)). According to experimental data, the increasing order of microbial inhibition by the extract is as follows: *Staphylococcus aureus*, *Bacillus subtilis*, and *Klebsiella pneumoniae*, based on the Nyquist diameter.

The  $R_{ct}$  values indicate that plant inhibitors were confined to the outermost layer of mild steel, acting as a controlled protective barrier, retarding the rate of the corrosion process. Electrochemical impedance data revealed that plant extracts effectively mitigated the development of microbial biofilms over the metal surface. Based on  $R_{ct}$  data, it was concluded that *Staphylococcus aureus* + *Reullia tuberosa* reported low current consumption, followed by *Klebsiella pneumoniae* + *Reullia tuberosa*, and finally *Bacillus Subtilis* in the extracts [27]. The green inhibitors act as an additional layer of protection, regulating and delaying the corrosion process on the outermost layer of mild steel specimens [36]. Positively charged plant extract (inhibitor) molecules, through the exchange of electrons, established interactions (adsorption) with negatively charged metallic surfaces [37]. These green inhibitors minimize microbial adherence on the metal surface by reducing current consumption and corrosion rates and by forming protective layers [38]. Figure 5(a-c) represents the impedance analysis of *Reullia tuberosa*.

The development of microorganisms and their released components is associated with the formation of biofilms, which significantly impacts the double-layer capacitance ( $C_{dl}$ ) of a mild steel surface. Experimental data revealed that the capacitance development of the studies spans from  $1.4 \times 10^{-13}$  to  $5.2 \times 10^{-14}$  in all three categories of investigation. The biofilm development is closely associated with the reduction in the double-layer capacitance. The development of biofilms depends on the availability of nutrients and the synthesis of metabolites throughout bacterial growth [39]. Bacteria and their constituents constitute the majority of adsorption sites for mild steel. The double-layer capacitance becomes increasingly insensitive as the biofilm develops, suggesting that external factors other than the bacterial cell might influence the capacitance during evaluation [40]. Technically, a limited quantity of charge is stored in that localized zone, and the thickness of the double layer is determined by the electrolyte's characteristics and the experimental setup [41]. Experimental studies revealed that the plant extracts were able to inhibit, on average, above 80% with more than 75% surface coverage in all three categories.

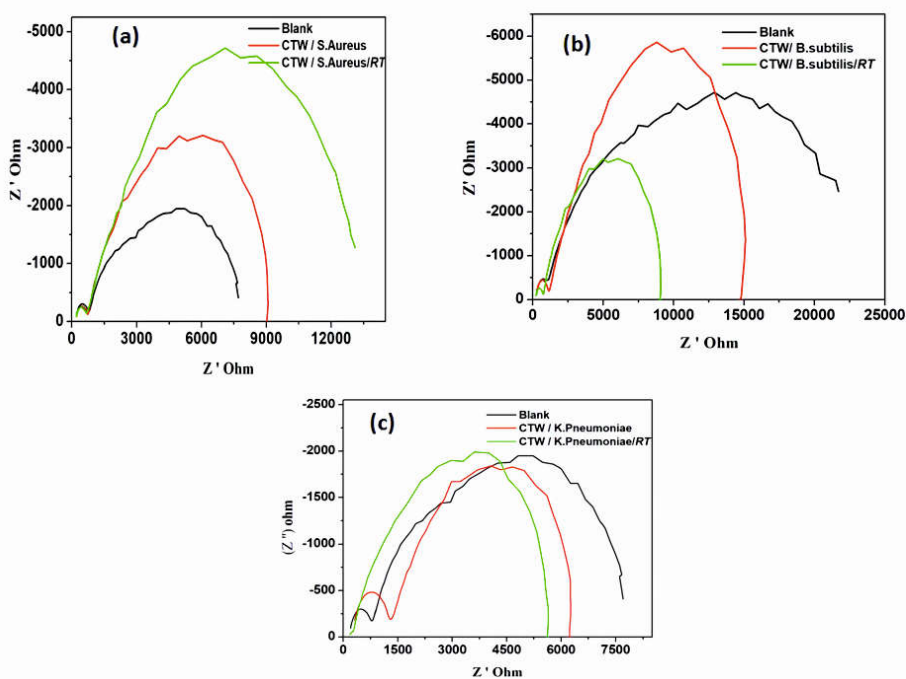


Figure 5. Impedance analysis of *Ruellia tuberosa* treatment of *S. aureus* (a), *B. subtilis* (b) and *K. pneumoniae* (c).

#### Tafel plots

Microbial corrosion is facilitated by certain bacterial strains' metabolic processes and the development of their biofilms. The antibacterial qualities of some plant extracts have been investigated; these properties assist in minimising biocorrosion [42]. Table 3(b) represents the polarisation parameters for mild steel in control, microbial (*S. aureus*, *B. subtilis*, *K. pneumoniae*), and inhibitor (*Ruellia tuberosa*) systems. Literature reports that the higher the corrosion potential,

the higher the rate of corrosion, and vice versa [43]. The potentiodynamic polarisation curves provided the Tafel parameters such as corrosion potential ( $E_{\text{corr}}$ ), corrosion current density ( $I_{\text{corr}}$ ), and cathodic and anodic Tafel slopes ( $\beta_a$ ,  $\beta_c$ ) [6]. A compound can only be regarded as either an anodic, cathodic, or mixed-type inhibitor based on its  $E_{\text{corr}}$  value [44]. Figure 6(a-c) represents *Ruellia tuberosa* plant extracts that effectively inhibited the rate of microbe-induced corrosion. In the case of *Ruellia tuberosa* plant extract treatment studies, it was observed that CTW induced higher corrosion compared to microbe-induced and microbe-assisted plant extract. The  $E_{\text{corr}}$  value demonstrated the fact that the microbial corrosion by *Staphylococcus aureus* and *Bacillus subtilis* was effectively inhibited by the plant extract, but the polarisation curve of *Klebsiella pneumonia* was more negative compared to CTW + *Klebsiella pneumonia* + plant extract. A high negative value warranted a higher corrosion rate based on the  $E_{\text{corr}}$  value. Moreover, the  $I_{\text{corr}}$  value of *Klebsiella pneumonia* is high compared to *Staphylococcus aureus* and *Bacillus subtilis*. Figure 6 (a-c) represents the polarisation curves of biocorrosion studies. The mild steel corrosion represented high negative values compared to other categories. Polarization resistance ( $R_p$ ) of the investigation demonstrated that plant extract mediated microbial corrosion was found to be low.

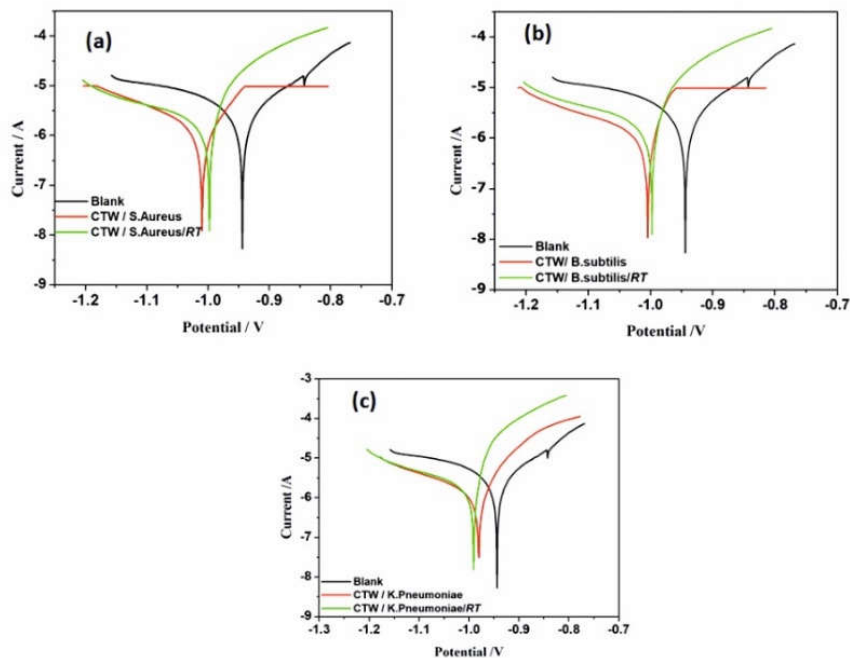


Figure 6. Corrosion and bio-corrosion studies mediated by *Ruellia tuberosa*.

Table 3(a). Impedance parameters derived from Nyquist plots.

Immersion of MS in systems	$R_s$	$R_{ct}$ (ohm cm <sup>2</sup> )	$C_{dl}$ (F / cm <sup>2</sup> )	$\theta$	IE %
Control	210.2	1000	$5.21 \times 10^{-14}$	--	--
<i>S. aureus</i>	215.7	8069.80	$7.78 \times 10^{-14}$	0.8761	87.61
<i>S. aureus</i> and <i>Ruellia tuberosa</i>	229.6	11207.60	$7.35 \times 10^{-14}$	0.9108	91.08
<i>B. subtilis</i>	230	8069.80	$7.35 \times 10^{-14}$	0.8761	87.61
<i>B. subtilis</i> and <i>Ruellia tuberosa</i>	273.6	11102.00	$6.01 \times 10^{-14}$	0.9099	90.99
<i>K. pneumoniae</i>	252.2	5000.00	$5.86 \times 10^{-14}$	0.8000	80.00
<i>K. pneumoniae</i> and <i>Ruellia tuberosa</i>	313.7	5574.00	$5.76 \times 10^{-14}$	0.8206	82.06

Table 3(b). Polarisation parameters for mild steel in control, microbial (*S. aureus*, *B. subtilis*, *K. pneumoniae*), and inhibitor (*Ruellia tuberosa*) systems.

Immersion of mild steel in systems	$-E_{corr}$ (V)	$I_{corr}$ (A / cm <sup>2</sup> )	$R_p$ ( $\Omega$ )	$\beta_a$ (V / dec)	$\beta_c$ (V / dec)
Control	0.945	$1.68 \times 10^{-5}$	5927	7.404	3.620
<i>S. aureus</i>	1.010	$4.48 \times 10^{-6}$	6000	1.075	4.993
<i>S. aureus</i> and <i>Ruellia tuberosa</i>	1.000	$4.31 \times 10^{-6}$	9378	7.607	3.158
<i>B. subtilis</i>	1.010	$4.42 \times 10^{-6}$	8927	7.404	3.620
<i>B. subtilis</i> and <i>Ruellia tuberosa</i>	1.010	$4.3 \times 10^{-6}$	15548	6.073	3.715
<i>K. pneumoniae</i>	0.980	$4.49 \times 10^{-6}$	9549	10.709	4.266
<i>K. pneumoniae</i> and <i>Ruellia tuberosa</i>	0.990	$4.35 \times 10^{-6}$	9549	8.091	3.601

### Weight loss

Metal solubility in the solution, influences corrosion metal instability and loses weight. The weight loss of specimens linearly decreases in the corrosion rate with the addition of inhibitors [45]. Phyto-constituents present in the extract has anti-microbial activity, thereby inhibiting microbial harbouring and adhesion on the external surface of the metal, subsequently mitigating biofilm formation and bio-corrosion [46]. After 21 days of exposure to green inhibitor (*Ruellia tuberosa* extract), the weight loss for *Staphylococcus aureus*, *Bacillus subtilis*, and *Klebsiella pneumoniae* was determined to be 0.015 g, 0.016 g, and 0.017 g, respectively, and corrosion rates in three categories were reported to be 3.2 mm/year, 3.4 mm/year, and 3.7 mm/year, respectively. The corrosion inhibition efficiencies were found to be 82.5, 80.6, and 79.8% for the respective systems after 21 days. Literature have reported that various factors such as phyto-constituents, extract concentration, extraction solvent, extraction temperature, mild steel coupon exposure duration and operating temperature play a vital role in difference in the corrosion inhibition efficiencies of plant extracts [47]. It was concluded from weight loss experiments that at an optimum plant extract concentration of 30 ppm, there was an inhibition of more than 70% on the biocorrosion of mild steel [48]. The Potent phytoconstituents of *Ruelliatuberosa* extract successfully mitigated microbial-induced corrosion, demonstrating its potential as a sustainable solution in controlling biocorrosion while promoting eco-friendly industrial applications [49-50].

## CONCLUSION

A potential solution to mitigate microbiological corrosion in various metals and environments is the utilization of green inhibitors. These naturally occurring inhibitors are non-toxic, affordable,

and possess long-term viability. Secondary metabolites present in green inhibitors make them a promising option for bio-corrosion control due to their antibacterial properties against a variety of gram-positive and gram-negative microorganisms. Green inhibitors serve as an eco-friendly alternative for preventing microbial corrosion, as they inhibit the growth of biofilms on metal surfaces. They offer a sustainable option compared to synthetic, toxic, and non-renewable commercial inhibitors. Various industrial and structural components are consistently impacted by microbially influenced corrosion (MIC). The mechanism and chemistry of pitting corrosion by microbes, along with the development of biofilms, constitute a complex and multifaceted process involving the release of numerous by-products by microbes and steel structures into the surrounding environment. SEM analysis revealed prominent scratches on the surface, indicating a significant relationship between corrosion patterns in localized areas of the metal's outermost layer. Corrosion products accumulate on an uneven corroded surface, attributed to the accumulation of microbial consortia metabolites. This accumulation leads to a modification of surface chemistry, transforming the structural composition of corrosive materials, increasing metallic surface porosity, and permeability. Functional groups in secondary metabolites of microbes facilitate the formation of biofilms over the metallic surface, as observed in FTIR analysis. Green inhibitors proved effective in controlling biofilm growth and metabolite accumulation. XRD graphs documented that green inhibitor effectively controlled the microbial growth products. GC-MS analysis of *Reullia tuberosa* revealed the presence of antimicrobial compounds. Nyquist plots and impedance investigations substantiated the role played by green inhibitors in controlling biocorrosion. The extensive use of conventional, harmful corrosion inhibitors in recent decades has prompted the exploration of eco-friendly inhibitors derived from inexpensive and environmentally friendly materials. The future of corrosion mitigation relies on discovering, identifying, and developing an efficient and sustainable formulation that inhibits microbial adherence to metallic surfaces and minimizes the corrosion process. A combinatorial approach integrating a comprehensive understanding of microbial chemistry, electrochemistry, and surface interactions is essential for developing a formulation with high inhibitory efficiency and minimal environmental impact.

#### ACKNOWLEDGMENTS

We would like to extend our heartfelt thanks to the Government College of Engineering, Salem, for giving us the chance to properly complete our research project. We extend our gratitude to the scientific staff members of the Department of Chemistry Laboratory for their invaluable assistance over the course of the experimental research.

#### *Authors' contribution*

R. Sharmil Suganya: Planning and conduction of experiments, result analysis and manuscript writing; Stanelybritto Maria Arul Francis: Conduction of experiments and result analysis; T. Venugopal: Editing the manuscript and manuscript writing.

#### *Funding*

No funding.

#### *Research content*

The research content of manuscript is original and has not been published elsewhere.

*Ethical approval*

No animals or living plants and/or injured during the study in associated environs.

*Conflict of interest*

The authors declare that there is no conflict of interest.

*Data availability*

Not applicable.

## REFERENCES

1. da Rocha Magalhães, L.; da Silva Alvarenga, R.F.; Resende, F.A.C.; da Silva, L.R.R.; Filho, W.W.B.; Franco, S.D. The synergy between corrosion and fatigue: Failure analysis of an aerator and a cooling tower. *J. Fail. Anal. Prev.* **2023**, *23*, 1803-1819.
2. Kokilaramani, S.; Al-Ansari, M.M.; Rajasekar, A.; Al-Khattaf, F.S.; Hussain, A.; Govarthanam, M. Microbial influenced corrosion of processing industry by re-circulating waste water and its control measures - A review. *Chemosphere* **2021**, *265*, 129075.
3. Telegdi, J.; Shaban, A.; Trif, L. Microbiologically influenced corrosion (MIC). *Trends Oil Gas Sci. Technol.* **2017**, 191-214.
4. Kuraimid, Z.K.; Majeed, H.M.; Jebur, H.Q.; Ahmed, T.S.; Jaber, O.S. Synthesis of new corrosion inhibitors with high efficiency in aqueous and oil phase for low carbon steel for missan oil field equipment. *Eurasian Chem. Commun.* **2021**, *3*, 860-871.
5. Kaya, F.; Solmaz, R.; Gecibesler, I.H. Adsorption and corrosion inhibition capability of *Rheum ribesroot* extract (Işgım) for mild steel protection in acidic medium: A comprehensive, surface characterization, synergistic inhibition effect, and stability study. *J. Mol. Liq.* **2023**, *372*, 121219.
6. Hossain, S.M.Z.; Razzak, S.A.; Hossain, M.M. Application of essential oils as green corrosion inhibitors. *Arab. J. Sci. Eng.* **2020**, *45*, 7137-7159.
7. Sezonov, G.D.; Joseleau-Petit, d'Ari. *Escherichia coli* physiology in Luria-Bertani broth. *J. Bacteriol.* **2007**, *189*, 8746-8749.
8. Aslam, M.Z.; Lin, X.; Li, X.; Yang, N.; Chen, L. Molecular cloning and functional characterization of CpMYC2 and CpBHLH13 transcription factors from winter sweet (*Chimonanthus praecox* L.). *Plants* **2020**, *9*, 785.
9. Balouiri, M.; Sadiki, M.; Ibsouda, S.K. Methods for in vitro evaluating antimicrobial activity: A review. *J. Pharm. Anal.* **2016**, *6*, 71-79.
10. Narenkumar, J.; Parthipan, P.; Usha Raja Nanthini, A.; Benelli, G.; Murugan, K.; Rajasekar, A. Ginger extract as green biocide to control microbial corrosion of mild steel. *3 Biotech* **2017**, *7*, 1-11.
11. Rathnakumar, S.S.; Noluthando, K.; Kulandaiswamy, A.J.; Rayappan, J.B.B.; Kasinathan, K.; Kennedy, J.; Maaza, M. Stalling behaviour of chloride ions: a non-enzymatic electrochemical detection of  $\alpha$ -endosulfan using CuO interface. *Sens. Actuators B: Chem.* **2019**, *293*, 100-106.
12. Nwigwe, U.S.; Mbam, S.O.; Umunakwe, R. Evaluation of *Carica papaya* leaf extract as a bio-corrosion inhibitor for mild steel applications in a marine environment. **2019**, *6*, 105107.
13. Agarry, S.E.; Oghenejoboh, K.M.; Aworanti, O.A.; Arinkoola, A.O. Biocorrosion inhibition of mild steel in crude oil-water environment using extracts of *Musa paradisiaca* peels, *Moringa oleifera* leaves, and *Carica papaya* peels as biocidal-green inhibitors: Kinetics and adsorption studies. *Chem. Eng. Commun.* **2019**, *206*, 98-124.

14. Anbarasi, K.; Sivakumar, V. Ultrasonic-assisted solvent extraction of phenolic compounds from *Opuntia ficus-indica* peel: PHYtochemical identification and comparison with Soxhlet extraction. *J. Food Process Eng.* 2019, 42, e131226.
15. Pal, M.K.; Lavanya, M. Microbial influenced corrosion: Understanding bioadhesion and biofilm formation. *J. Bio. Tribo. Corros.* **2022**, 8, 76.
16. Loto, C.A. Microbiological corrosion: Mechanism, control and impact—a review. *Int. J. Adv. Manuf. Technol.* **2017**, 92, 4241-4252.
17. Knisz, J.; Eckert, R.; Gieg, L.M.; Koerdt, A.; Lee, J.S.; Silva, E.R.; Skovhus, T.L.; An Stepec, B.A.; Wade, S.A. Microbiologically influenced corrosion—more than just microorganisms. *FEMS Microbiol. Rev.* **2023**, 47, 1-33.
18. Mohan, V.R.; Rajendrakumar, N.; Vasantha, K. GC-MS analysis of bioactive components of tubers of *Ruellia tuberosa* L. (Acanthaceae). *Am. J. Phytomedicine Clin. Ther.* **2014**, 2, 209-216.
19. Lin, Q.; Li, Y.; Sheng, M.; Xu, J.; Xu, X.; Lee, J.; Tan, Y. Antibiofilm effects of berberine-loaded chitosan nanoparticles against *Candida albicans* biofilm. *LWT Food Sci. Technol.* **2023**, 173, 114237.
20. da Silva, B. D.; Bernardes, P.C.; Pinheiro, P.F.; Fantuzzi, E.; Roberto, C.D. Chemical composition, extraction sources and action mechanisms of essential oils: Natural preservative and limitations of use in meat products. *Meat Sci.* **2021**, 176, 108463.
21. Caldwell, D.E.; Korber, D.R.; Lawrence, L.R. *Confocal Laser Microscopy and Digital Image Analysis in Microbial Ecology in Advances in Microbial Ecology*, Boston, MA: Springer US; **1992**; pp. 1-67.
22. Mohd Ali, M.K.F.B.; Abu Bakar, A.; Md. Noor, N.; Yahaya, N.; Ismail, M.; Rashid, A.S. Hybrid solivave technique for mitigating sulfate-reducing bacteria in controlling biocorrosion: A case study on crude oil sample. *Environ. Technol.* **2017**, 38, 2427-2439.
23. Albahri, M.B.; Barifcani, A.; Iglauer, S.; Lebedev, M.; O'Neil, C.; Salgar-Chaparro, S.J.; Machuca, L.L. Investigating the mechanism of microbiologically influenced corrosion of carbon steel using X-ray micro-computed tomography. *J. Mater. Sci.* **2021**, 56, 13337-13371.
24. Malek, T.J.; Chaki, S.H.; Deshpande, M.P. Structural, morphological, optical, thermal and magnetic study of mackinawite FeS nanoparticles synthesized by wet chemical reduction technique. *Phys. B: Condens. Matter.* **2018**, 546, 59-66.
25. Otton, L.M.; da Silva Campos, M.; Meneghetti, K.L.; Corção, G. Influence of twitching and swarming motilities on biofilm formation in *Pseudomonas* strains. *Arch. Microbiol.* **2017**, 199, 677-682.
26. Karthik, R.; Muthukrishnan, P.; Chen, S.M.; Jeyaprabha, B.; Prakash, P. Anti-corrosion inhibition of mild steel in 1 M hydrochloric acid solution by using *Tiliacora acuminata* leaves extract. *Int. J. Electrochem. Sci.* **2015**, 10, 3707-3725.
27. AlSalhi, M. S.; Devanesan, S.; Rajasekar, A.; Kokilaramani, S. Characterization of plants and seaweeds-based corrosion inhibitors against microbially influenced corrosion in a cooling tower water environment. *Arab. J. Chem.* **2023**, 16, 104513.
28. Amajida, H.; Purwoko, T.; Susilowati, A. Antibacterial activity of ethanolic and n-hexane extracts of *Ruellia tuberosa* leaves against *Escherichia coli* and *Bacillus subtilis* bacteria. *Asian J. Nat. Prod. Biochem.* **2019**, 17, 69-80.
29. Das, S.; Ghosh, A.; Mukherjee, A. Nanoencapsulation-based edible coating of essential oils as a novel green strategy against fungal spoilage, mycotoxin contamination, and quality deterioration of stored fruits: An overview. *Front. Microbiol.* **2021**, 12, 768414.
30. Videla, H. *Manual of biocorrosion*. Routledge; **2018**.
31. Ech-chihbi, E.; Adardour, M.; Ettahiri, W.; Salim, R.; Ouakki, M.; Galai, M.; Baouid, A.; Taleb, M. Surface interactions and improved corrosion resistance of mild steel by addition of new triazolyl-benzimidazolone derivatives in acidic environment. *J. Mol. Liq.* **2023**, 387, 122652.

32. Cai, T.; Zhang, Y.; Wang, N.; Zhang, Z.; Lu, X.; Zhen, G. Electrochemically active microorganism's sense charge transfer resistance for regulating biofilm electroactivity, spatio-temporal distribution, and catabolic pathway. *Chem. Eng. J.* **2022**, 442, 136248.
33. Pais, M.; Rao, P. Electrochemical, spectroscopic and theoretical studies for acid corrosion of zinc using glycogen. *Chem. Pap.* **2021**, 75, 1387-1399.
34. Xu, D.; Li, Y.; Gu, T. Mechanistic modelling of biocorrosion caused by biofilms of sulfate reducing bacteria and acid producing bacteria. *Bioelectrochemistry* **2016**, 110, 52-58.
35. Karn, S.K.; Fang, G.; Duan, J. *Bacillus sp.* acting as dual role for corrosion induction and corrosion inhibition with carbon steel (CS). *Front. Microbiol.* **2017**, 8, 2038.
36. Farh, H.M.H.; Seghier, M.E.A.B.; Zayed, T. A comprehensive review of corrosion protection and control techniques for metallic pipelines. *Eng. Fail. Anal.* **2023**, 143, 106885.
37. Preethi Kumari, P.; Shetty, P.; Rao, S.A. Electrochemical measurements for the corrosion inhibition of mild steel in 1 M hydrochloric acid by using an aromatic hydrazide derivative. *Arab. J. Chem.* **2017**, 10, 653-663.
38. Narenkumar, J.; Parthipan, P.; Madhavan, J.; Murugan, K.; Marpu, S.B.; Suresh, A.K.; Rajasekar, A. Bioengineered silver nanoparticles as potent anti-corrosive inhibitor for mild steel in cooling towers. *Environ. Sci. Pollut. Res.* **2018**, 25, 5412-5420.
39. Permech, S.; Lau, K.; Duncan, M. Characterization of biofilm formation and coating degradation by electrochemical impedance spectroscopy. *Coat.* 2019, 9, 518.
40. Fojt, J.; Průchová, E.; Hybášek, V. Electrochemical impedance response of the nanostructured Ti-6Al-4V surface in the presence of *S. aureus* and *E. coli*. *J. App. Electrochem.* **2023**, 53, 2153-2167.
41. Kim, T.; Kang, J.; Lee, J.-H.; Yoon, J. Influence of attached bacteria and biofilm on double-layer capacitance during biofilm monitoring by electrochemical impedance spectroscopy. *Water Res.* **2011**, 45, 4615-4622.
42. Victoria, S.N.; Sharma, A.; Manivannan, R. Metal corrosion induced by microbial activity – Mechanism and control options. *J. Indian Chem. Soc.* **2021**, 98, 100083.
43. Caldoná, E.B.; Al Christopher, C.; Mangadlao, J.D.; Lim, K.J.A.; Pajarito, B.B.; Advincula, R.C. On the enhanced corrosion resistance of elastomer-modified polybenzoxazine/graphene oxide nanocomposite coatings. *React. Funct. Polym.* **2018**, 123, 10-19.
44. Olasunkanmi, L.O.; Obot, I.B.; Kabanda, M.M.; Ebenso, E.E. Some quinoxalin-6-yl derivatives as corrosion inhibitors for mild steel in hydrochloric acid: experimental and theoretical studies. *J. Phys. Chem. C* **2015**, 119, 16004-16019.
45. Rao, P.; Mulky, L. Microbially influenced corrosion and its control measures: A critical review. *J. Bio-Tribo-Corros.* **2023**, 9, 57.
46. Briggs, W.F.; Stanley, H.O.; Okpokwasili, G.C.; Immanuel, O.M.; Ugboma, C.J.; Serrano, M. Biocorrosion inhibitory potential of aqueous extract of *Phyllanthus amarus* against acid producing bacteria. *J. Adv. Biol. Biotechnol.* **2019**, 22, 1-8.
47. Murungji, P.I.; Sulaimon, A.A. Ideal corrosion inhibitors: a review of plant extracts as corrosion inhibitors for metal surfaces. *Corros. Rev.* **2022**, 40, 127-136.
48. Geethapriyan, T.; Palani, I.A.; Singh, M.K.; Rai, D.K.; Shanmuga Priyan, V.G.; Subbu, S.K. Post-processing of wire arc additive manufactured stainless steel 308L to enhance compression and corrosion behavior using laser shock peening process. *J. Mater. Eng. Perform.* **2024**, 33, 9267-9281.
49. Kumar, M.; Tamang, S. K.; Thanigaivelan, R.; Dabi, M. Study of wettability behavior of water nanodroplets on platinum surface by molecular dynamics simulation. *Surf. Eng. Appl. Electrochem.* **2024**, 60, 50-57.
50. Hermonson, R.; Thanigaivelan, R.; Kavaya, V.; Rathinasamy, K.; Jagadeesha, T. Performance of electrochemically deposited hydroxyapatite on textured 316L SS for applications in biomedicine. *Surf. Eng.* **2023**, 39, 882-891.